

AIP | The Journal of Chemical Physics

Vector properties in photodissociation: Quantum treatment of the correlation between the spatial anisotropy and the angular momentum polarization of the fragments

Laurens D. A. Siebbeles, Michèle GlassMaujean, Oleg S. Vasyutinskii, J. Alberto Beswick, and Octavio Roncero

Citation: *J. Chem. Phys.* 100, 3610 (1994); doi: 10.1063/1.466402

View online: <http://dx.doi.org/10.1063/1.466402>

View Table of Contents: <http://jcp.aip.org/resource/1/JCPSA6/v100/i5>

Published by the [American Institute of Physics](http://www.aip.org).

Additional information on J. Chem. Phys.

Journal Homepage: <http://jcp.aip.org/>

Journal Information: http://jcp.aip.org/about/about_the_journal

Top downloads: http://jcp.aip.org/features/most_downloaded

Information for Authors: <http://jcp.aip.org/authors>

ADVERTISEMENT

Instruments for advanced science

Gas Analysis



- dynamic measurement of reaction gas streams
- catalysis and thermal analysis
- molecular beam studies
- dissolved species probes
- fermentation, environmental and ecological studies

Surface Science



- UHV TPD
- SIMS
- end point detection in ion beam etch
- elemental imaging - surface mapping

Plasma Diagnostics



- plasma source characterization
- etch and deposition process
- reaction kinetic studies
- analysis of neutral and radical species

Vacuum Analysis



- partial pressure measurement and control of process gases
- reactive sputter process control
- vacuum diagnostics
- vacuum coating process monitoring

contact Hiden Analytical for further details

HIDEN
ANALYTICAL

info@hideninc.com
www.HidenAnalytical.com

CLICK to view our product catalogue 

Vector properties in photodissociation: Quantum treatment of the correlation between the spatial anisotropy and the angular momentum polarization of the fragments

Laurens D. A. Siebbeles

LURE, Laboratoire CNRS, MEN, CEA, Centre Universitaire Paris-Sud, 91405 Orsay, France

Michèle Glass-Maujean

Laboratoire de Spectroscopie Hertzienne de l'École Normale Supérieure et de l'Université Pierre et Marie Curie, Associé au CNRS, 4 Pl. Jussieu, 75252 Paris Cedex 05, France

Oleg S. Vasyutinskii

Laboratoire de Spectroscopie Hertzienne de l'École Normale Supérieure et de l'Université Pierre et Marie Curie, Associé au CNRS, 4 Pl. Jussieu, 75252 Paris Cedex 05, France and A. F. Ioffe Physico-Technical Institute, Academy of Sciences of Russia, 194021 St. Petersburg, Russia

J. Alberto Beswick

LURE, Laboratoire CNRS, MEN, CEA, Centre Universitaire Paris-Sud, 91405 Orsay, France

Octavio Roncero

Instituto de Matemáticas y Física Fundamental, CSIC, Serrano 123, 28006 Madrid, Spain

(Received 23 July 1993; accepted 9 November 1993)

The dependence of the angular momentum polarization (orientation and alignment) of the fragments on the direction of ejection \mathbf{k} , is studied quantum mechanically for molecular photodissociation into two fragments of which one carries an angular momentum \mathbf{j} . Explicit expressions in terms of the transition matrix elements for electronic excitation into the final dissociative states are given in the axial-recoil limit and for different photon polarizations. The importance of interference effects due to coherent excitation of dissociative states with different helicity quantum numbers (the projection Ω of \mathbf{j} on the recoil direction \mathbf{k}) is stressed. It is shown that not only absolute magnitudes but also relative phases of individual transition matrix elements can be determined separately if the spatial anisotropy of the angular momentum polarization is measured.

I. INTRODUCTION

The study of vector properties in molecular photodissociation processes has received considerable experimental and theoretical attention lately¹⁻⁴ as a mean to obtain the most detailed information on the fragmentation dynamics. It is possible, for instance, to measure the distribution among magnetic sublevels $m \equiv j_Z$, corresponding to the projection of the angular momentum \mathbf{j} of a photofragment on the space-fixed Z axis (usually chosen parallel to the photon polarization vector \mathbf{e} for linear polarization and to the direction of propagation of the photon for circular or unpolarized light, see Fig. 1). This so-called angular momentum polarization of the fragments corresponds to a determination of the correlation between the vectors \mathbf{j} and \mathbf{Z} . In the simplest experimental situations the degree of polarization of the fragments is characterized by the orientation and alignment, which are related to the first and second moments of the m distribution, i.e., to $\langle j_Z \rangle$ and $\langle j_Z^2 \rangle$, respectively.⁵⁻¹²

Another vector property is the angular distribution of the photofragments in space, i.e., the correlation between the recoil direction \mathbf{k} of the fragments and the space-fixed \mathbf{Z} vector. In many experiments the $[\mathbf{j}, \mathbf{Z}]$ and $[\mathbf{k}, \mathbf{Z}]$ correlations have been measured independently from each other. Thus, orientation and alignment ($[\mathbf{j}, \mathbf{Z}]$ correlation) have very often been measured averaged over all directions of

ejection, while the angular distribution ($[\mathbf{k}, \mathbf{Z}]$ correlation) has been determined irrespective of the angular momentum polarization of the fragments. These measurements provide a wealth of crucial information concerning both the symmetries of the excited states and the dynamics of the half-collision process. However, as has been stressed by Houston and collaborators,¹³ the most detailed information on the photofragmentation process is obtained by determination of the correlation between \mathbf{j} and \mathbf{k} . This intrinsic $[\mathbf{j}, \mathbf{k}]$ correlation can be determined by measurement of the angular momentum polarization of the photofragments as a function of the direction of the recoil vector \mathbf{k} of the fragments. This can be performed by analysis of sub-Doppler line shapes obtained by laser-induced fluorescence (LIF) spectroscopy.^{2,12,13}

In a seminal paper,¹² Dixon provided the general theoretical determination of the $[\mathbf{j}, \mathbf{k}]$ correlation from the analysis of these Doppler-resolved line shapes. For linearly polarized light the correlation is defined by a number of bipolar moments of the translational and rotational angular distributions. In his paper, Dixon has provided the explicit equations which allow the determination of the bipolar moments from the polarization dependence of the Doppler profiles. He has also given an interpretation of the bipolar moments in terms of a semiclassical description of the fragmentation dynamics and some particular examples of the application of this treatment. As has been pointed

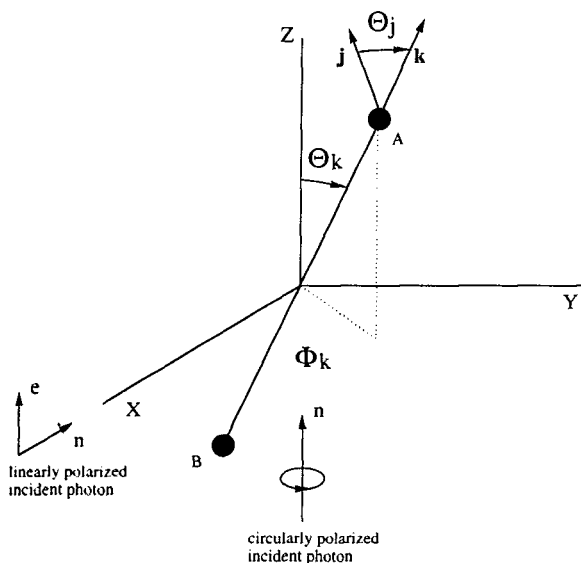


FIG. 1. Space-fixed reference frame used to establish Eqs. (14), (17)–(19), (22), and (30). n is the direction of propagation of the incident light.

out by Dixon in Sec. V of his paper,¹² the bipolar moments can in principle be calculated by use of the general quantum theory of photodissociation dynamics and a knowledge of the involved potential energy surfaces and transition dipole moments. This full quantum treatment of vector properties is necessary when the angular momenta involved are not large or when it is important to have explicit expressions for vector correlations in terms of photodissociation amplitudes which can be calculated by the use of scattering or half-collision theories.^{10,11} It is the purpose of this work to provide such a quantum treatment.

The formalism used is an extension of that in Ref. 11, where only the integrated angular momentum polarization of the fragments was considered. The problem is conceptually related to the spin and ion angular momentum polarization studies in photoionization.^{14–16} Photofragmentation into two fragments of which one carries an angular momentum \mathbf{j} is considered. Direct photodissociation of an initially randomly oriented molecule is assumed and the axial recoil approximation is used. Explicit expressions are provided for linearly polarized incident light and also for excitation with circularly or unpolarized light. The important case where several dissociative states with different helicity quantum numbers (the projection Ω of \mathbf{j} on the recoil direction \mathbf{k}) are excited coherently,¹¹ is discussed in detail. As expected, vector correlations as a function of the recoil direction of the fragments provide information which would be very difficult to extract from scalar properties. In particular, it is demonstrated that angularly resolved orientation and alignment can determine the individual absolute magnitudes as well as the relative phases of the transition matrix elements.

The organization of the paper is as follows. In Sec. II the excitation matrix for direct photodissociation is given in terms of the state multipoles. The detail of the calcula-

tions are given in Appendix A. In Sec. III the general results of Sec. II are used to explicitly calculate the differential cross section for photodissociation and the angular momentum polarization of the fragments. Section IV is devoted to the conclusions. Finally, the relationship between the quantum expressions and the semiclassical bipolar moments defined in Ref. 12 is given in Appendix B.

II. ANGULAR-DEPENDENT EXCITATION MATRIX AND STATE MULTIPOLES

We consider a photodissociation process producing two fragments of which one carries an angular momentum \mathbf{j} different from zero. For cases where the two fragments A and B have angular momentum different from zero, $\mathbf{j} = \mathbf{j}_A + \mathbf{j}_B$ and a final transformation is needed in order to calculate the vector correlations of \mathbf{j}_A and \mathbf{j}_B from those of \mathbf{j} .^{10,11} In first-order perturbation theory for electric dipole transitions the differential excitation matrix for one-photon fragmentation of an initially randomly oriented molecule, can be written as⁸

$$\sigma_{m'm}^{(j)}(\Theta_k, \Phi_k) = \frac{4\pi^2\omega}{c} \sum_{M_i} \frac{1}{2J_i+1} \langle \Psi_{j m'; \mathbf{k}} | \mathbf{d} \cdot \mathbf{e} | \Psi_{J_i M_i} \rangle \times \langle \Psi_{J_i M_i} | \mathbf{d} \cdot \mathbf{e}^* | \Psi_{j m; \mathbf{k}} \rangle, \quad (1)$$

where ω is the frequency of the incident light, \mathbf{e} its polarization vector, and \mathbf{d} the electric dipole operator. In Eq. (1) $\Psi_{J_i M_i}$ is the wave function of the initial molecular state with angular momentum J_i and projection M_i on the space-fixed Z axis. Finally, the dissociative wave function $\Psi_{j m; \mathbf{k}}$ in Eq. (1) describes the two photofragments flying apart with momentum $\hbar\mathbf{k}$ and direction specified by the polar angles Θ_k and Φ_k (see Fig. 1).

The partial differential cross section to produce fragments with a specific angular momentum \mathbf{j} and component m along the space-fixed Z axis, is given by the diagonal elements of the excitation matrix $\sigma_{mm}^{(j)}(\Theta_k, \Phi_k)$ defined in Eq. (1). However, to calculate the cross section for production of fragments with a component m along another axis the full excitation matrix $\sigma_{m'm}^{(j)}(\Theta_k, \Phi_k)$ is needed. This is the case in double excitation experiments where the photofragments are detected by LIF, for instance. The excitation matrix elements $\sigma_{m'm}^{(j)}$ for $m' \neq m$ describe the coherence between states with different quantum numbers m . In general there may be additional quantum numbers in the problem which may be excited coherently. In the present work only the coherences between magnetic sublevels m are considered. For convenience the superscript (j) will be dropped in the notation of the excitation matrix elements $\sigma_{m'm}$.

The plane-wave function $\Psi_{j m; \mathbf{k}}$ in Eq. (1) can be expressed in terms of the spherical harmonics Y_{lm_l} according to¹⁷

$$\Psi_{j m; \mathbf{k}} = \sum_{lm_l} \Psi_{j m; lm_l} Y_{lm_l}^*(\Theta_k, \Phi_k). \quad (2)$$

The quantum number l corresponds to the angular momentum associated to the relative motion of the centers of

mass of the two photofragments (orbital angular momentum), with m_l being its projection on the space-fixed Z axis. Since it is more convenient to calculate the matrix elements of the dipole operator \mathbf{d} in a body-fixed frame with the z axis along the vector \mathbf{R} joining the two centers of mass of the photofragments, the wave function $\Psi_{j_m, \mathbf{k}}$ is expressed in terms of molecule-fixed wave functions $\Psi_{j\Omega JM}$ (see Appendix A). J is the total angular momentum with projection Ω (the helicity quantum number) on the body-fixed z axis and M on the space-fixed Z axis. This quantum number becomes a good quantum number at infinite separation where the body-fixed z axis become parallel to \mathbf{R} . Since l is perpendicular to \mathbf{R} , Ω is also the projection of \mathbf{j} on the recoil direction. The quantum number Ω can, for instance, correspond to the projection of the electronic angular momentum. For a polyatomic molecule the nuclear rotation also contributes to the projection Ω .

It is convenient to express the excitation matrix elements $\sigma_{m'm}(\Theta_k, \Phi_k)$ in terms of the angular momentum polarization moments (state multipoles) $T_{KQ}(\Theta_k, \Phi_k)$, which are the spherical tensors of rank K and component Q defined by^{7,8}

$$T_{KQ}(\Theta_k, \Phi_k) = \sum_{m'm} (-1)^{j-m} (2K+1)^{1/2} \times \begin{pmatrix} j & K & j \\ -m & Q & m' \end{pmatrix} \sigma_{m'm}(\Theta_k, \Phi_k), \quad (3a)$$

$$\sigma_{m'm}(\Theta_k, \Phi_k) = \sum_{KQ} (-1)^{j-m} (2K+1)^{1/2} \times \begin{pmatrix} j & K & j \\ -m & Q & m' \end{pmatrix} T_{KQ}(\Theta_k, \Phi_k). \quad (3b)$$

The probability to produce the photofragment with an angular momentum \mathbf{j} in the direction (Θ_k, Φ_k) , i.e., the differential cross section, is then directly related to $T_{00}(\Theta_k, \Phi_k)$ and the other vector properties are related to the multipoles $T_{KQ}(\Theta_k, \Phi_k)$ with $K > 0$.

By combining Eqs. (1)–(3) and applying the properties of the $3-j$ symbols in a way analogous to Ref. 11, it is found that the differential polarization moment can be written as (see Appendix A)

$$T_{KQ}(\Theta_k, \Phi_k) = \frac{2\pi^{3/2}\omega}{c} \sum_{qq'} \sum_{PS} (-1)^q (2P+1)^{1/2} (2S+1)^{1/2} \times [Y_S(\mathbf{k}) \otimes E_P(\mathbf{e})]_{KQ} \begin{pmatrix} 1 & 1 & P \\ q' & -q & q-q' \end{pmatrix} \times \begin{pmatrix} P & S & K \\ q'-q & 0 & q-q' \end{pmatrix} f_K(q, q'), \quad (4)$$

where $[Y_S(\mathbf{k}) \otimes E_P(\mathbf{e})]$ denotes the tensor product

$$[Y_S(\mathbf{k}) \otimes E_P(\mathbf{e})]_{KQ} = \sum_{ps} (-1)^{S-P+Q} (2K+1)^{1/2} \times \begin{pmatrix} S & P & K \\ s & p & -Q \end{pmatrix} Y_{Ss}(\Theta_k, \Phi_k) E_{Pp}(\mathbf{e}). \quad (5)$$

The function $E_{Pp}(\mathbf{e})$ depends only on the polarization of the incident light and is given by^{6,8}

$$E_{Pp}(\mathbf{e}) = (2P+1)^{1/2} \sum_{\eta\eta'} (-1)^{\eta} e_{\eta} e_{\eta'}^* \begin{pmatrix} 1 & 1 & P \\ \eta & -\eta' & -p \end{pmatrix}, \quad (6)$$

with $P=0, 1, 2$. The functions $f_K(q, q')$ in Eq. (4) are defined by

$$f_K(q, q') = \sum_{\Omega_i} (-1)^{j+\Omega_i-q} \begin{pmatrix} j & j & K \\ -\Omega & \Omega' & q'-q \end{pmatrix} \times M_{j\Omega, \Omega'} (M_{j\Omega, \Omega'})^* \quad (7)$$

with $\Omega = \Omega_i - q$ and $\Omega' = \Omega_i - q'$, and $M_{j\Omega, \Omega'}$ being the transition dipole matrix elements defined by

$$M_{j\Omega, \Omega'} = \sum_{j'} \int dR \Phi_{\Omega_i}^{(j)'}(R) \langle \varphi_{\Omega_i} | (\mathbf{d})_q | \varphi_{j'\Omega} \rangle \Phi_{j\Omega, j'\Omega'}^{(j)}(R), \quad (8)$$

where φ designates basis functions describing the internal states of the fragments at infinite R . The $\Phi(R)$ functions in Eq. (8) describe the relative radial motion of the fragments and can be calculated using scattering or half-collision techniques.^{10,18,19}

The $f_K(q, q')$ functions defined by Eq. (7) contain all the information on the transition dipole moments and fragmentation dynamics via the products of the transition matrix elements $M_{j\Omega, \Omega'}$ of the dipole operator between the initial bound and final dissociative states as defined by Eq. (8). For this reason they may be called the *dynamical functions* for direct photodissociation. It should be noted from Eq. (8) that q can only take the values 0 or ± 1 , corresponding to parallel and perpendicular electronic transitions, respectively. Also, if $q \neq q'$ in Eq. (7) then $\Omega \neq \Omega'$, and this corresponds to a simultaneous coherent excitation of continua with different helicities. These terms are responsible for interference effects in vector properties.^{3,10,11} They cannot appear in the differential cross section which is related to the $K=0$ moment, but they are important in the determination of the orientation ($K=1, 3, \dots$) and in the alignment ($K=2, 4, \dots$). In the diatomic case, they may arise from the simultaneous excitation of a Σ and a Π electronic state or from the excitation of the two components ± 1 of a Π state.³

The dynamical functions $f_K(q, q')$ defined by Eq. (7) obey the following symmetry rules:²⁰

$$f_K(q, q') = (-1)^K f_K(-q, -q');$$

$$f_K(q, q') = (-1)^{q-q'} f_K^*(q', q). \tag{9}$$

One consequence of these properties is that odd K moments cannot be produced via parallel transitions²¹ for which $q=q'=0$ since according to the first of Eqs. (9), $f_K(0,0)=0$ for K odd.

Equations (4) to (8) give our final expressions for the angular-dependent state multipoles $T_{KQ}(\Theta_k, \Phi_k)$ in terms of the transition matrix elements of the dipole operator, for all possible incident photon polarizations and for any choice of the space-fixed reference frame. From the $3-j$ coefficients in Eq. (7) it follows that $T_{KQ}(\Theta_k, \Phi_k)$ can be different from zero for $K=0, 1, \dots, 2j$. Also, from the $3-j$ coefficient in Eq. (5) it is seen that Q can take any integer value from $-K$ to K . On the contrary, if the $T_{KQ}(\Theta_k, \Phi_k)$ are integrated over the dissociation angles (Θ_k, Φ_k) , only the $S=0$ term contributes to Eq. (4) and in that case from Eqs. (5) and (6) one obtains the well-known result that the integrated polarization moments T_{KQ} are nonzero only for $K=P=0, 1$, and 2 .⁸

Using Eq. (4) into Eq. (3b) it is possible to obtain the angular-dependent quantum excitation matrix $\sigma_{m'm}(\Theta_k, \Phi_k)$ for direct photodissociation of an initially randomly oriented molecule. It is possible, starting from Eq. (3b), to establish the connection between this quantum theory and the semiclassical treatment of Ref. 12 which was given in terms of bipolar moments. This connection is presented in Appendix B.

In addition to the space-fixed multipoles T_{KQ} given by Eq. (4), it is possible to define body-fixed multipoles \mathcal{T}_{KQ} by the transformations

$$\mathcal{T}_{KQ}(\Theta_k, \Phi_k) = \sum_{Q'} D_{QQ'}^K(\Phi_k, \Theta_k, 0) T_{KQ'}(\Theta_k, \Phi_k), \tag{10a}$$

$$T_{KQ}(\Theta_k, \Phi_k) = \sum_{Q'} D_{QQ'}^{K*}(\Phi_k, \Theta_k, 0) \mathcal{T}_{KQ'}(\Theta_k, \Phi_k). \tag{10b}$$

Actually, these multipoles refer to a frame with the z axis along the recoil direction of the fragments \mathbf{k} . Asymptotically however, i.e., for infinite R , the \mathbf{k} becomes rigorously parallel to \mathbf{R} . Anyway, within the framework of the axial recoil approximation used in this work \mathbf{k} and \mathbf{R} are always parallel (see Fig. 1).

From Eq. (10) and using the Clebsch–Gordan series⁸ to perform the summations over S and s in Eqs. (4) and (5) one obtains

$$\mathcal{T}_{KQ}(\Theta_k, \Phi_k) = \frac{\pi\omega}{c} \sum_{qq'} \sqrt{2K+1} (-1)^{K+q'} f_K(q, q') \sum_P (2P+1)^{1/2} \times \mathcal{E}_{PQ}(\mathbf{e}, \Theta_k, \Phi_k) \begin{pmatrix} 1 & 1 & P \\ q' & -q & -Q \end{pmatrix}, \tag{11}$$

where

$$\mathcal{E}_{PQ}(\mathbf{e}, \Theta_k, \Phi_k) = \sum_P E_{Pp}(\mathbf{e}) D_{pQ}^P(\Phi_k, \Theta_k, 0) \tag{12}$$

are the components of the $E_{Pp}(\mathbf{e})$ polarization functions defined in Eq. (6) in the body-fixed coordinate frame. We note from Eq. (11) that the components Q of the angular momentum polarization moments $\mathcal{T}_{KQ}(\Theta_k, \Phi_k)$ in the body-fixed frame are restricted to the values $Q=0, \pm 1, \pm 2$. This is expected for one-photon electric dipole transitions for which only parallel ($q=0$) or perpendicular electronic transitions ($q=\pm 1$) are allowed.

Using the $\mathcal{T}_{KQ}(\Theta_k, \Phi_k)$ multipoles the excitation matrix in the body-fixed frame can then be obtained by

$$\sigma_{\Omega'\Omega}(\Theta_k, \Phi_k) = \sum_{KQ} (-1)^{j-\Omega} (2K+1)^{1/2} \times \begin{pmatrix} j & K & j \\ -\Omega & Q & \Omega' \end{pmatrix} \mathcal{T}_{KQ}(\Theta_k, \Phi_k) \tag{13a}$$

which is the equivalent of Eq. (3b) in the space-fixed frame. Actually, the space-fixed $\sigma_{m'm}(\Theta_k, \Phi_k)$ and the body-fixed $\sigma_{\Omega'\Omega}(\Theta_k, \Phi_k)$ excitation matrices are related by the transformation

$$\sigma_{m'm}(\Theta_k, \Phi_k) = \sum_{\Omega\Omega'} D_{m'\Omega'}^j(\Phi_k, \Theta_k, 0) \sigma_{\Omega'\Omega}(\Theta_k, \Phi_k) D_{m\Omega}^{j*}(\Phi_k, \Theta_k, 0). \tag{13b}$$

If the space-fixed Z axis is chosen to coincide with the polarization vector for linearly polarized incident light and with the propagation direction of the light for circularly polarized or unpolarized light (see Fig. 1), then $p=0$ in Eq. (6). With this choice of space-fixed coordinates it can be shown, from Eqs. (4) and (5), that after angular integration only the T_{K0} multipoles can be different from zero. This in turn implies that integration over all dissociation directions makes the excitation matrix $\sigma_{m'm}$ diagonal.

Since the $T_{K0}(\Theta_k, \Phi_k)$ multipoles determined the diagonal elements of the excitation matrix $\sigma_{m'm}$, it is useful to provide their explicit expressions in terms of the dynamical functions $f_K(q, q')$ defined in Eq. (7). From Eqs. (4) and (5) it is found

$$\begin{aligned}
T_{K0}(\Theta_k, \Phi_k) = & \frac{\pi\omega}{4c} \sqrt{2K+1} (\{[f_K(0,0) + 2f_K(1,1)]^2 [1 + (-1)^K] [1 + \beta_K P_2(\cos \Theta_k)] + 2af_K(1,1) \\
& \times [1 - (-1)^K] \cos \Theta_k\} D_{00}^{K*}(\Phi_k, \Theta_k, 0) - 2\sqrt{2} \operatorname{Re}\{f_K(1,0)\} \sin \Theta_k [-a[1 - (-1)^K] \\
& + b[1 + (-1)^K] \cos \Theta_k\} D_{01}^{K*}(\Phi_k, \Theta_k, 0) + bf_K(1, -1) [1 + (-1)^K] \sin^2 \Theta_k D_{02}^{K*}(\Phi_k, \Theta_k, 0)), \quad (14)
\end{aligned}$$

where a and b are coefficients which depend only on the state of polarization of the incident light. They are listed in Table I for linear, circular, and unpolarized photons. The Wigner rotation matrix elements $D_{mm'}^{K*}(\Phi_k, \Theta_k, 0)$ appearing in Eq. (14) are presented explicitly in Table II for $K=0, 1$, and 2 . The anisotropy parameter β_K in Eq. (14) is given by

$$\beta_K = \frac{2[f_K(0,0) - f_K(1,1)]}{f_K(0,0) + 2f_K(1,1)} \quad (15a)$$

for linearly polarized light, and by

$$\beta_K = -\frac{[f_K(0,0) - f_K(1,1)]}{f_K(0,0) + 2f_K(1,1)} \quad (15b)$$

for circularly polarized or unpolarized light. For $K=0$, Eq. (15) yields the well-known anisotropy parameter describing the angular distribution of the photofragments.¹⁷

$T_{K0}(\Theta_k, \Phi_k)$ as given by Eq. (14) consists of three terms containing the Wigner rotation matrix elements $D_{00}^K(\Phi_k, \Theta_k, 0)$, $D_{01}^K(\Phi_k, \Theta_k, 0)$, and $D_{02}^K(\Phi_k, \Theta_k, 0)$. The coefficient of D_{00}^K involves $f_K(q, q')$ functions with $q=q'$. From the definition of the dynamical $f_K(q, q')$ functions given in Eq. (7) it is seen that this corresponds to a sum of incoherent terms of the form $|M_{j\Omega, \Omega'}|^2$. Actually, a comparison of Eqs. (14) and (10b) reveals that the coefficient of D_{00}^K in Eq. (14) is just the body-fixed multipole \mathcal{T}_{K0} . Its angular dependence is given by $[1 + \beta_K P_2(\cos \Theta_k)]$ for even K and by $\cos \Theta_k$ for odd K . For odd K , however, it will be different from zero only for circular polarization (see Table I). The two other terms in Eq. (14) are proportional to $D_{01}^K(\Phi_k, \Theta_k, 0)$ and $D_{02}^K(\Phi_k, \Theta_k, 0)$, and involve $f_K(q, q')$ functions with $q - q' = 1$ and 2 , respectively. From Eq. (7) it is seen that they correspond to terms of the form $M_{j\Omega, \Omega'} (M_{j\Omega, \Omega'})^*$ with $\Omega - \Omega' = \pm 1$ and ± 2 , respectively. Therefore, in order to have a contribution from these terms it is necessary to have simultaneous (coherent) excitation of final dissociative states with different helicities. As stressed above, these terms give rise to interference effects which are important in many cases. In particular, they were invoked as a possible mechanism to explain the anom-

ously high orientation of the CN fragments found experimentally in the photodissociation of ICN.^{4(a),4(b)} They are also known to be important in determining the polarization of fragment fluorescence.³ From Eq. (10b) it is seen that the coefficients of $D_{01}^K(\Phi_k, \Theta_k, 0)$ and $D_{02}^K(\Phi_k, \Theta_k, 0)$ in Eq. (14) are the body-fixed multipoles \mathcal{T}_{KQ} with $Q = \pm 1$ and ± 2 , respectively. It is also clear from Eq. (14) that the angular dependence of the term proportional to D_{01}^{K*} is very different for even and odd K . The term proportional to D_{02}^{K*} , on the other hand, is nonzero only for the multipoles with an even K .

The general conclusions presented above are not only valid for $K=1$ and $K=2$ but also for the higher order state multipoles ($K=3, 4, \dots, 2j$). The multipoles of rank $K > 2$ vanish after integration over the recoil direction and thus they can be obtained only from angular resolved studies. However, the higher polarization moments are of interest. They provide more detailed information on the spatial distribution of j .

III. DIFFERENTIAL CROSS SECTION AND ANGULAR MOMENTUM POLARIZATION OF THE FRAGMENTS

In this section we provide the explicit expressions for the differential cross section, as well as for the orientation and the alignment of the fragments angular momentum for the most usual choice of the space-fixed frame, namely the one in which the Z axis is in the direction of the polarization vector for linearly polarized incident light and in the direction of the propagation direction of the light for circularly polarized or unpolarized light (see Fig. 1).

A. Differential cross section

From Eq. (3a) it is easy to show that the differential cross section $\sigma(\Theta_k, \Phi_k)$ for production of a photofragment with a specific angular momentum j is proportional to the zero-order multipole $T_{00}(\Theta, \Phi)$,

$$\sigma(\Theta_k, \Phi_k) \equiv \sum_m \sigma_{mm}(\Theta_k, \Phi_k) = \sqrt{2j+1} T_{00}(\Theta, \Phi). \quad (16)$$

TABLE I. Polarization-dependent coefficients a and b in Eqs. (14), (22), (24), and (30).

Polarization	a	b
Linear	0	-2
Unpolarized	0	1
Circular	-1	1

TABLE II. Wigner rotation functions $D_{0m}^K(\Theta_k, \Phi_k, 0)$ appearing in Eq. (14).

$D_{0m}^K(\Theta_k, \Phi_k, 0)$	$K=0$	$K=1$	$K=2$
$m=0$	1	$\cos \Theta_k$	$(3 \cos^2 \Theta_k - 1)/2$
$m=1$...	$1/\sqrt{2} \sin \Theta_k$	$\sqrt{3/2} \sin \Theta_k \cos \Theta_k$
$m=2$	$\sqrt{3/8} \sin^2 \Theta_k$

TABLE III. The values of polarization momenta $T_{KQ}(\Theta, \Phi)$ divided by $\pi\omega/c$ for different angles Θ and $\Phi=0$ from which the functions $f_K(q, q')$ can be obtained straightforwardly.

	$\Theta=0$	$\Theta=\pi/4$	$\Theta=\pi/2$	Polarization
T_{00}	$f_0(0,0)$...	$f_0(1,1)$	linear
T_{00}	$f_0(1,1)$...	$f_0(0,0)/2$	circular
T_{10}	$-\sqrt{3}f_1(1,1)$...	$-\sqrt{3} \operatorname{Re}[f_1(1,0)]$	circular
T_{11}	0	$-i\sqrt{3}/2 \operatorname{Im}[f_1(1,0)]$	0	linear
T_{20}	$\sqrt{5}f_2(1,1)$	circular
T_{20}	$\sqrt{5}f_2(0,0)$	$-\frac{\sqrt{5}}{2} \left\{ \frac{f_2(0,0)+f_2(1,1)}{4} - \sqrt{3} \operatorname{Re}[f_2(1,0)] - \frac{\sqrt{6}}{8} f_2(1,-1) \right\}$	$-\frac{\sqrt{5}}{2} \left\{ f_2(1,1) + \frac{\sqrt{6}}{2} f_2(1,-1) \right\}$	linear

Then with the choice of the space-fixed frame of Fig. 1, Eq. (14) provides the celebrated expression¹⁷

$$\sigma(\Theta_k, \Phi_k) = \frac{\sigma_0}{4\pi} [1 + \beta_0 P_2(\cos \Theta_k)] \quad (17)$$

with

$$\sigma_0 = \frac{4\pi^2\omega}{3c} [f_0(0,0) + f_0(1,1) + f_0(-1,-1)] \quad (18)$$

and

$$\beta_0 = \frac{2[f_0(0,0) - f_0(1,1)]}{f_0(0,0) + 2f_0(1,1)} \quad \text{for linearly polarized light,} \quad (19a)$$

$$\beta_0 = -\frac{[f_0(0,0) - f_0(1,1)]}{f_0(0,0) + 2f_0(1,1)} \quad \text{for circularly polarized or unpolarized light.} \quad (19b)$$

In the case of a pure parallel or perpendicular transition, Eqs. (19) give the well-known limiting values $\beta_0'' = 2$ and $\beta_0' = -1$ for linearly polarized light and $\beta_0'' = -1$ and $\beta_0' = \frac{1}{2}$ for circularly polarized or unpolarized light. For linearly polarized incident light $\sigma(\Theta_k, \Phi_k)$ is proportional to $f_0(0,0)$ at $\Theta_k=0$, and $f_0(-1,-1) + f_0(1,1)$ at $\Theta_k=\pi/2$. The dynamical functions $f_0(0,0)$ and $f_0(1,1)$ can thus be obtained from a measurement of the differential cross section at $\Theta_k=0$ and $\Theta_k=\pi/2$ (see also Table III). However, the functions $f_0(0,0)$ and $f_0(1,1)$ as defined by Eq. (7) depend only on $|M_{j\Omega,\Omega'}|^2$. Thus a measurement of the differential cross section cannot provide any information on the phases of the transition matrix elements $M_{j\Omega,\Omega'}$.

B. Orientation

The angular-dependent orientation of the photofragment angular momentum \mathbf{j} is defined by^{7,8}

$$O_Q^{(1)}(\mathbf{j}) = \frac{1}{\sqrt{j(j+1)}} \operatorname{Re}\{\langle j_Q^{(1)} \rangle\} \quad (20)$$

with $j_0^{(1)} = j_Z$ and $j_{\pm 1}^{(1)} = \mp(1/\sqrt{2})j_{\pm}$, where $j_{\pm} = (j_x \pm ij_y)$. From Eqs. (3) one gets

$$O_Q^{(1)}(\mathbf{j}) = \left[\frac{(2j+1)}{3} \right]^{1/2} \operatorname{Re} \left\{ \frac{T_{1Q}(\Theta_k, \Phi_k)}{\sigma_0} \right\}. \quad (21)$$

If again, the space-fixed Z axis is chosen as in Fig. 1, Eq. (4) provides

$$T_{11}(\Theta_k, \Phi_k) = \frac{\pi\omega}{c} \frac{\sqrt{6}}{2} \cos \Theta_k \sin \Theta_k \exp(i\Phi_k) \{ -af_1(1,1) + a \operatorname{Re}[f_1(1,0)] + ib \operatorname{Im}[f_1(1,0)] \}, \quad (22a)$$

$$T_{10}(\Theta_k, \Phi_k) = a \frac{\pi\omega}{c} \sqrt{3} \{ f_1(1,1) \cos^2 \Theta_k + \operatorname{Re}[f_1(1,0)] \sin^2 \Theta_k \}, \quad (22b)$$

$$T_{1-1}(\Theta_k, \Phi_k) = -T_{11}^*(\Theta_k, \Phi_k), \quad (22c)$$

where a and b are the polarization dependent coefficients listed in Table I. A number of conclusions follow from Eqs. (22) and the values that a and b take for different polarizations. One is that orientation along the space-fixed Z axis cannot be obtained with linear polarized or unpolarized light since $a=0$ for those cases.⁸ On the other hand, orientation along the space-fixed X or Y axis can be obtained by the use of linearly polarized light if there is a coherent superposition of a parallel and a perpendicular transition, i.e., if $f_1(1,0) \neq 0$. This is a well-known fact in the context of spin polarization.^{15,16}

Except for the terms involving $f_1(1,0)$, Eqs. (22) are identical to the results given for circularly polarized light in Ref. 22. As noted above, $f_1(0,0)$ which involves only parallel transitions, does not contribute to the orientation. On the other hand, $f_1(1,1)$ which involves perpendicular transitions, does contribute to the orientation. It is interesting to note, however, that $f_1(1,1)$ as given in Eq. (7), vanishes if $\Omega=\Omega'=0$. Thus from Eqs. (21) and (22) it is concluded that in order to produce orientation of a photofragment angular momentum \mathbf{j} at least one perpendicular transition to a state with $\Omega \neq 0$ has to be involved in the photofragmentation process.

The angular dependence of the expectation values $\langle j_Y \rangle$ and $\langle j_Z \rangle$ as obtained from Eqs. (20) to (22) are presented by polar graphs in Fig. 2 for circularly polarized light. Figure 2(a) represents $\langle j_Y \rangle \sim \cos \Theta_k \sin \Theta_k \sin \Phi_k$ for a pure perpendicular transition. It is seen that $\langle j_Y \rangle = 0$ for photofragments flying apart along the Z axis or in the

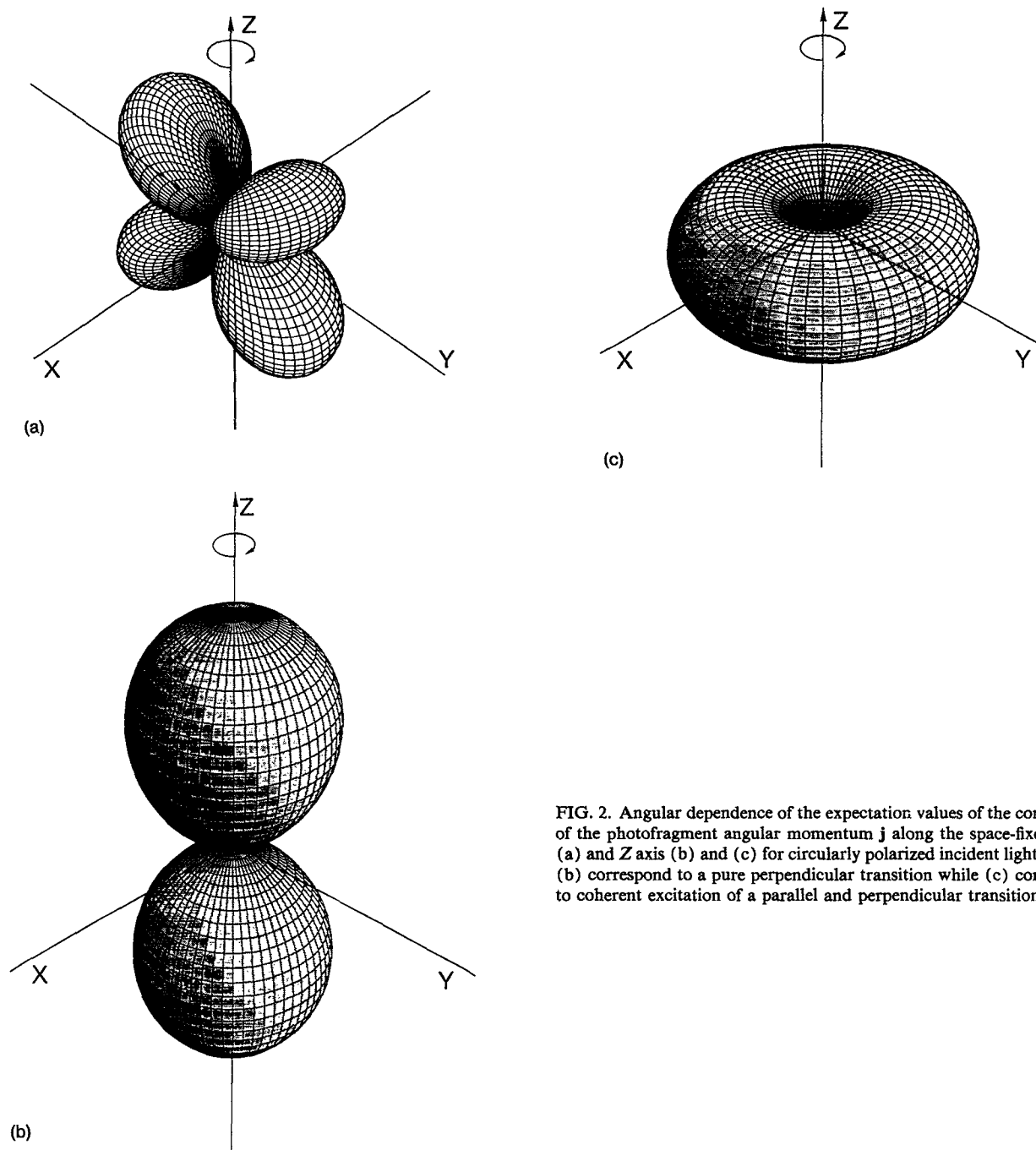


FIG. 2. Angular dependence of the expectation values of the components of the photofragment angular momentum \mathbf{j} along the space-fixed Y axis (a) and Z axis (b) and (c) for circularly polarized incident light. (a) and (b) correspond to a pure perpendicular transition while (c) corresponds to coherent excitation of a parallel and perpendicular transition.

XY plane. The maximum value of $\langle j_Y \rangle$ is reached for fragments moving in the YZ plane at an angle $\Theta_k = \pi/4$ or $3\pi/4$. In Fig. 2(b) a similar polar graph corresponding to $\langle j_Z \rangle \sim \cos^2 \Theta_k$ for a pure perpendicular transition is presented. In this case $\langle j_Z \rangle$ is equal to zero for dissociations in the XY plane and reaches a maximum if the fragments move along the Z axis. The angular dependence of $\langle j_Z \rangle$ for a coherent excitation of a parallel and perpendicular transition is proportional to $\sin^2 \Theta_k$ and is presented in Fig. 2(c). From this figure it is clear that coherent excitation gives a maximum of $\langle j_Z \rangle$ for fragments flying apart in the XY plane while $\langle j_Z \rangle = 0$ for fragments moving along the Z axis.

Physical insight on the results given in Eqs. (22) can be obtained by writing the photofragment angular momentum as [see Fig. 3(a)]

$$\mathbf{j} = j_{\parallel} \mathbf{k} + j_{\perp} (\mathbf{k} \times \mathbf{Z}) + j'_{\perp} [(\mathbf{k} \times \mathbf{Z}) \times \mathbf{k}]. \quad (23)$$

Thus, j_{\parallel} is the component of \mathbf{j} along \mathbf{k} , j_{\perp} is the component perpendicular to the plane containing \mathbf{k} and the laboratory Z axis, while j'_{\perp} is the component lying on the same plane and perpendicular to \mathbf{k} . Using Eqs. (20)–(23) it is found that

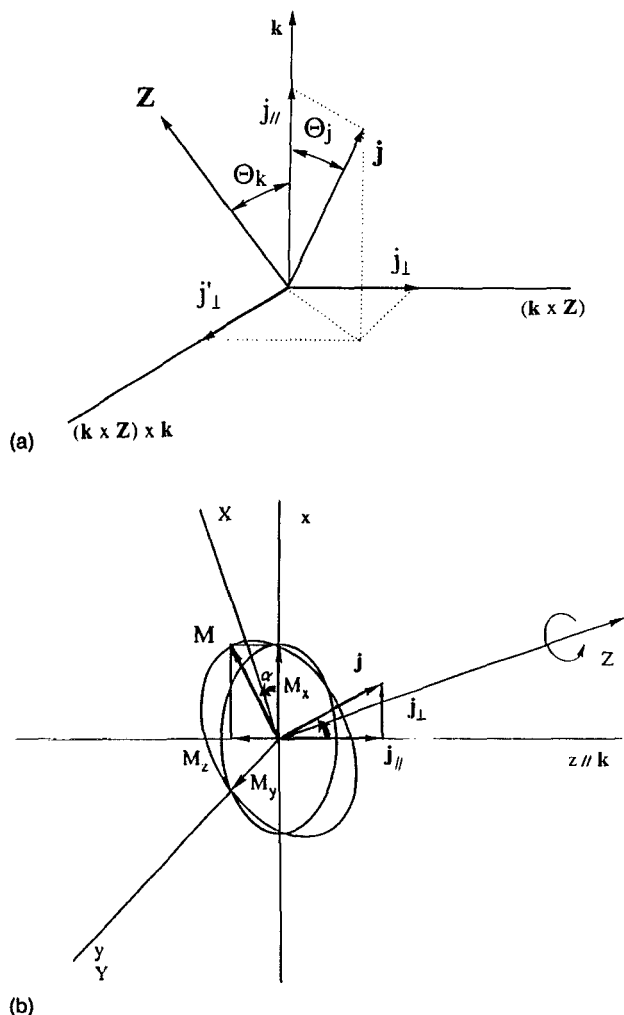


FIG. 3. (a) Components of the photofragment angular momentum j in the body-fixed frame. (b) Components of the transition dipole moment M and the classical angular momentum.

$$\langle j_{\parallel} \rangle = a \frac{\pi\omega}{c} \frac{\sqrt{j(j+1)}}{\sigma_0} f_1(1,1) \cos \Theta_k, \quad (24a)$$

$$\langle j_{\perp} \rangle = b \frac{\pi\omega}{c} \frac{\sqrt{j(j+1)}}{\sigma_0} \text{Im}\{f_1(1,0)\} \cos \Theta_k \sin \Theta_k, \quad (24b)$$

$$\langle j'_{\perp} \rangle = a \frac{\pi\omega}{c} \frac{\sqrt{j(j+1)}}{\sigma_0} \text{Re}\{f_1(1,0)\} \sin \Theta_k \quad (24c)$$

which show that a pure perpendicular transition [$f_1(1,1) \neq 0$] produces a component of the fragments angular momentum parallel to the recoil direction, while a coherent superposition of a parallel and a perpendicular transition [$f_1(1,0) \neq 0$] produces a component perpendicular to the recoil direction.

These results can also be obtained by a classical treatment of the interaction of light and matter following the arguments presented in Ref. 23 for the simple case of a superposition of a parallel Σ - Σ and a perpendicular Σ - Π transition in a diatomic molecule. The time-dependent transition dipole moment M is defined by M

$= \langle \Psi_{jm';k} | d | \Psi_{JM'} \rangle$ after evolution of the dissociating system. The components of M in the body-fixed frame, as defined in Fig. 3(b), can be written for circularly polarized incident light as

$$M_x = M_{\Pi} \exp(-i\phi_{\Pi}) \cos(\Theta_k) \exp(-i\omega t) / \sqrt{2} \\ = M \cdot (k \times Z) \times Z, \quad (25a)$$

$$M_y = iM_{\Pi} \exp(-i\phi_{\Pi}) \exp(-i\omega t) / \sqrt{2} = M \cdot (k \times Z), \quad (25b)$$

$$M_z = -M_{\Sigma} \exp(-i\phi_{\Sigma}) \exp(-i\omega t) / \sqrt{2} = M \cdot k. \quad (25c)$$

The phases ϕ_{Σ} and ϕ_{Π} are due to the evolution of the system during the dissociation, which causes a dephasing between the dissociative channels populated by the parallel transition and the perpendicular transition. The classical angular momentum introduced by the transition can be written as

$$j_c = \left(M \times \frac{dM}{dt} \right) \frac{1}{M^2}. \quad (26)$$

From Eqs. (25) and (26) it is straightforward to obtain

$$(j_c)_{\parallel} = \frac{\omega}{M^2} M_{\Pi}^2 \cos(\Theta_k), \quad (27a)$$

$$(j_c)_{\perp} = \frac{\omega}{M^2} M_{\Sigma} M_{\Pi} \sin(\phi_{\Pi} - \phi_{\Sigma}) \sin(\Theta_k) \cos(\Theta_k), \quad (27b)$$

$$(j_c)'_{\perp} = \frac{\omega}{M^2} M_{\Sigma} M_{\Pi} \cos(\phi_{\Pi} - \phi_{\Sigma}) \sin(\Theta_k). \quad (27c)$$

Comparison of Eqs. (24) and (27) shows that the classical model describing the interaction of circularly polarized light and the molecule gives essentially the same results as the quantum-mechanical treatment. Note that for linearly polarized light the classical angular momentum is given by Eq. (27b) after replacing Θ_k by $\Theta_k - \pi/2$. The other components of the classical angular momentum are zero for linearly polarized light.

Equation (26) shows that the transition dipole moment M must rotate in order to obtain a nonzero angular momentum. In a pure parallel transition the vector M is oscillating along the body-fixed z axis and does not rotate. In a pure perpendicular transition induced by circularly polarized light the vector M rotates in a plane perpendicular to the internuclear axis, creating an angular momentum along the internuclear axis. If both parallel and perpendicular transitions are induced by linearly polarized light, the dephasing of the transition moments due to the dissociation causes the vector M to rotate in the plane containing the internuclear axis and the laboratory Z axis. This gives rise to an angular momentum perpendicular to that plane. For circularly polarized light the vector M produced by a coherent excitation of parallel and perpendicular transitions is not rotating anymore in a plane perpen-

dicular to the internuclear axis, but is tilted by an angle α [see Fig. 3(b)]. The direction of the angular momentum is changed accordingly such that

$$\tan \alpha = \frac{(j_{sc})'_\perp}{(j_{sc})_\parallel} = \frac{M_\Sigma \sin(\Theta_k) \cos(\phi_\Pi - \phi_\Sigma)}{M_\Pi \cos(\Theta_k)}.$$

The component $(j_{sc})_\perp$ can be explained analogously.

Equations (22) and (24) demonstrate that the function $f_1(1,0)$ can be obtained by measuring the angular dependence of the orientation of the angular momentum \mathbf{j} . This enables one to determine the relative phases of the transition matrix elements for parallel and perpendicular transitions. The dissociation angles and polarizations of the incident light needed for a straightforward determination of the $f_1(q, q')$ functions are given in Table III. Using circularly polarized light for instance, the real part of $f_1(1,0)$ can be obtained from a measurement of the orientation of \mathbf{j} along the space-fixed Z axis for fragments flying apart with $\Theta_k = \pi/2$. The imaginary part of $f_1(1,0)$ on the other hand, can be determined from the orientation of the components of \mathbf{j} in the XY plane by using linearly incident polarized light and detecting fragments at $\Theta_k = \pi/4$.

If Eqs. (22) are integrated over the dissociation recoil direction (Θ_k, Φ_k) , T_{11} and T_{1-1} vanish and T_{10} is the only nonzero multipole of rank 1. Thus a measurement of

the integrated orientation gives information only on a linear combination of $f_1(1,1)$ and $\text{Re}\{f_1(1,0)\}$. On the contrary, angular resolved studies of the orientation allow determination of $f_1(1,1)$, $\text{Re}\{f_1(1,0)\}$, and $\text{Im}\{f_1(1,0)\}$.

C. Alignment

The alignment $A_Q^{(2)}(j)$ of the photofragment angular momentum \mathbf{j} is defined as⁸

$$A_Q^{(2)}(j) = \frac{\sqrt{6}}{j(j+1)} \text{Re}(\langle j_Q^{(2)} \rangle) \quad (1)$$

with $j_{\pm 2}^{(2)} = \frac{1}{2}j_\pm^2$, $j_{\pm 1}^{(2)} = \mp \frac{1}{2}j_\pm(2j_z \pm 1)$, and $j_0^{(2)} = (1/2)(3j_z^2 - j^2)$ where $j_\pm = (j_x \pm ij_y)$. From Eqs. (3) and (28) one gets

$$A_Q^{(2)}(j) = \left[\frac{(2j-1)(2j+1)(2j+3)}{5j(j+1)} \right]^{1/2} \text{Re} \left\{ \frac{T_{2Q}(\Theta_k, \Phi_k)}{\sigma_0} \right\} \quad (2)$$

If the space-fixed Z axis is chosen as in Fig. 1, from Eq. (4) it follows that the $T_{2Q}(\Theta_k, \Phi_k)$ multipoles take the form

$$T_{22}(\Theta_k, \Phi_k) = \frac{\pi\omega}{c} \frac{\sqrt{30}}{8} \left\{ \frac{2}{3} [f_2(0,0) + 2f_2(1,1)] [1 + \beta_2 P_2(\cos \Theta_k)] - \frac{4\sqrt{3}}{3} [b \text{Re}\{f_2(1,0)\} \cos^2 \Theta_k + ai \text{Im}\{f_2(1,0)\}] + \frac{b}{\sqrt{6}} f_2(1,-1) [1 + \cos^2 \Theta_k] \right\} \sin^2 \Theta_k \exp(2i\Phi_k), \quad (3)$$

$$T_{21}(\Theta_k, \Phi_k) = -\frac{\pi\omega}{c} \frac{\sqrt{30}}{4} \left\{ \frac{2}{3} [f_2(0,0) + 2f_2(1,1)] [1 + \beta_2 P_2(\cos \Theta_k)] - \frac{2\sqrt{3}}{3} [b \text{Re}\{f_2(1,0)\} [2 \cos^2 \Theta_k - 1] - ai \text{Im}\{f_2(1,0)\}] - \frac{b}{\sqrt{6}} f_2(1,-1) \sin^2 \Theta_k \right\} \sin \Theta_k \cos \Theta_k \exp(i\Phi_k), \quad (3)$$

$$T_{20}(\Theta_k, \Phi_k) = \frac{\pi\omega}{c} \frac{\sqrt{5}}{2} \left\{ \left[\frac{2}{3} [f_2(0,0) + 2f_2(1,1)] [1 + \beta_2 P_2(\cos \Theta_k)] \right] \left[\frac{3 \cos^2 \Theta_k - 1}{2} \right] + \{ b 2\sqrt{3} \text{Re}\{f_2(1,0)\} \sin \Theta_k \cos \Theta_k + \left[b \frac{\sqrt{6}}{4} f_2(1,-1) \sin^2 \Theta_k \right] \sin^2 \Theta_k \right\}, \quad (3)$$

$$T_{2-1}(\Theta_k, \Phi_k) = -T_{21}^*(\Theta_k, \Phi_k), \quad (30d)$$

$$T_{2-2}(\Theta_k, \Phi_k) = T_{22}^*(\Theta_k, \Phi_k). \quad (30e)$$

As in Eqs. (14) and (22) the polarization dependent coefficients a and b in Eqs. (30) are those given in Table I. The appearance of $f_2(0,0)$ and $f_2(1,1)$ in Eqs. (30) indicate that both parallel and perpendicular electronic transitions give rise to alignment of \mathbf{j} .

The factors between $\{ \}$ in Eq. (30c) are proportional to the multipoles of rank 2 in the body-fixed coordinate frame. For instance, the first term in Eq. (30c) involves incoherent excitations of parallel and perpendicular transitions, i.e., containing $f_2(0,0)$ and $f_2(1,1)$ dynamical functions, is due to the component j_\parallel of \mathbf{j} , i.e., the component parallel to the body-fixed z axis [see Fig. 3(a)]. The third term, involving the function $f_2(1,-1)$, is due to components of \mathbf{j} perpendicular to the body-fixed z axis. The second term, involving the coherent excitation of para-

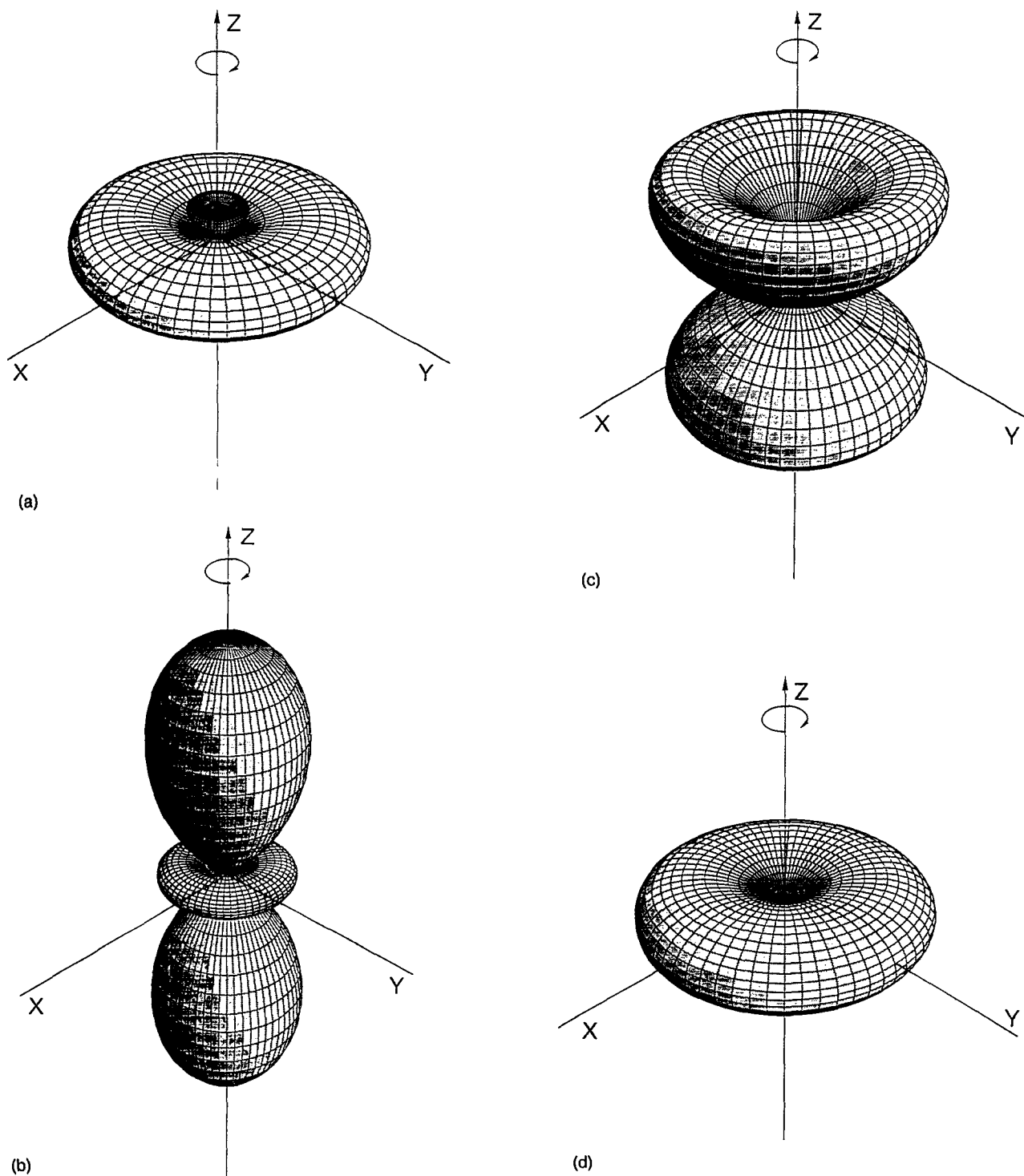


FIG. 4. Angular dependence of the alignment of the photofragment angular momentum j along the space-fixed Z axis, for circularly polarized incident light. The space-fixed coordinate frame is the one defined in Fig. 1. The graphs represent the contribution to the alignment of a pure parallel transition (a), a pure perpendicular transition (b), and a coherence excitation involving $|q-q'|=1$ (c) and $|q-q'|=2$ (d).

and perpendicular transitions [dynamical function $f_2(1,0)$], is due to components of j both parallel and perpendicular to the body-fixed z axis.

The angular dependence of these different terms in Eq. (30c) are represented by the polar plots of Fig. 4 for the case of circularly polarized incident light. Since $Q=0$ in Eq. (30c), the graphs correspond to the alignment of j

along the space-fixed Z axis. Figure 4(a) presents the contribution of a pure parallel transition [term involving $f_2(0,0)$ in Eq. (30c)] while Fig. 4(b) presents the contribution of the term involving $f_2(1,1)$. It is seen that they both vanish at the magic angle where $3 \cos^2 \Theta_k - 1 = 0$. Figure 4(a) shows that for a parallel transition the alignment is zero if the photofragments are flying apart along

the Z axis, and that maximum alignment is reached for fragments with recoil directions in the XY plane. For the $f_2(1,1)$ contribution, the alignment is maximum for fragments moving along the Z axis, see Fig. 4(b). Figure 4(c) represents the alignment due to the coherent term involving $\text{Re}[f_2(1,0)]$ in Eq. (30c). This contribution vanishes for dissociation along the Z axis and in the XY plane. Actually, it gives maximum alignment for $\Theta_k = \pi/4$. Finally, in Fig. 4(b) the contribution to the alignment of the term involving the function $f_2(1,-1)$ is presented. This contribution gives zero alignment for fragments flying apart along the Z axis and its maximum contribution is for fragments moving in the XY plane.

As in the case of orientation, angular resolved studies of the degree of alignment provide information about the incoherent and coherent excitation processes separately, which cannot be obtained from the alignment integrated over all final dissociation directions. Table III presents the dissociation angles and polarizations of the incident light which are needed for a straightforward determination of the dynamical $f_2(q,q')$ functions. In addition to the information which can be obtained from the differential cross section and the degree of orientation, it is seen from Table III that $f_2(1,-1)$ can be determined by a combination of the alignment along the Z axis measured at $\Theta_k = 0, \pi/4$, and $\pi/2$ with linearly polarized light.

IV. CONCLUSIONS

The spatial anisotropy of the angular momentum polarization (orientation and alignment) of a photofragment has been studied quantum mechanically for one-photon electric dipole transitions. Photodissociation into two fragments, one of which carries a nonzero angular momentum \mathbf{j} , was considered. The process was assumed to be direct and the axial recoil approximation has been used. The final expressions for the polarization moments do not rely on a particular choice of coordinate frame or on the polarization of the incident light. The cross section for production of a photofragment with both the magnitude and the component on a particular quantization axis of its angular momentum specified, can be obtained from these polarization moments. Explicit expressions for the angular resolved degree of orientation and alignment are obtained in terms of the transition matrix elements for electronic excitation into final dissociative states. The results of the quantal treatment are also discussed by comparison with those obtained by treating the radiation-matter interaction classically.

It is shown that determination of the angular resolved polarization of the photofragments provides detailed information on the photodissociation dynamics, which cannot be obtained from the integrated data. In particular, it is demonstrated that in the case of coherent excitation of continua with different helicity quantum numbers (the projection of \mathbf{j} on the recoil direction) it is possible to extract both the absolute values and the relative phases of the transition matrix elements.

The relationship between the quantum theory of $[\mathbf{k}, \mathbf{j}]$ correlations and Dixon's semiclassical treatment¹² in terms of bipolar harmonics, has been established. This is very useful since the semiclassical limit is valid in the limit of j much larger than the total angular momentum J ; a situation very often encountered in the dissociation of polyatomic molecules where \mathbf{j} corresponds to the rotation of the fragments.

The calculations presented in this paper assume that the molecule is initially isotropic, i.e., randomly oriented in space. In the future, it will be important to develop similar treatments for initially oriented molecules for which experimental results are becoming available.^{4(c)}

APPENDIX A: DERIVATION OF THE GENERAL EXPRESSIONS

The derivation of the general expression for the multipoles T_{KQ} given in Eq. (4) will be outlined. When Eq. (2) is introduced into Eq. (1), the excitation matrix becomes

$$\begin{aligned} \sigma_{m'm} = & \frac{4\pi^2\omega}{c} \sum_{M_i} \sum_{lm_i} \sum_{l'm'_i} \frac{1}{2J_i+1} \\ & \times Y_{lm_i}^*(\Theta_k, \Phi_k) Y_{l'm'_i}(\Theta_k, \Phi_k) \\ & \times \langle \Psi_{jm'l'm'_i} | \mathbf{d} \cdot \mathbf{e} | \Psi_{JM_i} \rangle \langle \Psi_{JM_i} | \mathbf{d} \cdot \mathbf{e}^* | \Psi_{jmlm_i} \rangle. \end{aligned} \quad (\text{A1})$$

It is more convenient to calculate the matrix elements of the dipole operator \mathbf{d} in the body-fixed coordinate frame. Therefore the wave function Ψ_{jmlm_i} is expressed in terms of wave functions for which the component Ω of the total angular momentum \mathbf{J} on the z axis is well-defined at infinite internuclear separation. This can be done according to¹⁹

$$\begin{aligned} \Psi_{jmlm_i} = & \sum_{\Omega JM} (-1)^{M-\Omega} (2l+1)^{1/2} (2J+1)^{1/2} \\ & \times \begin{pmatrix} j & l & J \\ \Omega & 0 & -\Omega \end{pmatrix} \begin{pmatrix} j & l & J \\ m & m_l & -M \end{pmatrix} \Psi_{j\Omega JM}. \end{aligned} \quad (\text{A2})$$

The wave function $\Psi_{j\Omega JM}$ is written as

$$\Psi_{j\Omega JM} = \frac{1}{R} \sum_{j'\Omega'} \Phi_{j\Omega, j'\Omega'}^J(R) W_{j'\Omega'}^{JM}(\mathbf{R}, \mathbf{r}), \quad (\text{A3})$$

where \mathbf{r} indicates all the internal coordinates (electronic, vibrational, and rotational) of the fragments. The basis functions $W_{j'\Omega'}^{JM}(\mathbf{R}, \mathbf{r}_{mf})$ are given by

$$W_{j'\Omega'}^{JM}(\mathbf{R}, \mathbf{r}_{mf}) = \sqrt{\frac{2J+1}{4\pi}} D_{M\Omega}^{j'*}(\Phi_k, \Theta_k, 0) \varphi_{j'\Omega'}(r; R). \quad (\text{A4})$$

The Wigner function $D_{M\Omega}^{j'*}(\Phi_R, \Theta_R, 0)$ describes the rotation of the molecule and $\varphi_{j'\Omega'}$ is an intramolecular

wave function, which at infinite R corresponds to an eigenfunction of the fragments. Substitution of Eqs. (A2)–(A4) into Eq. (A1) yields

$$\begin{aligned} \sigma_{m'm} = & \frac{4\pi^2\omega}{c} \sum_{M_i} \sum_{lm_i} \sum_{lm'_i} \sum_{\Omega JM} \sum_{\Omega' J' M'} \sum_{\Omega_i \Omega'_i} \sum_{\eta \eta'} (-1)^{2J_i - \Omega_i - \Omega'_i + M + M' - \Omega - \Omega'} e_{\eta}^* e_{\eta'} \\ & \times (2l+1)^{1/2} (2l'+1)^{1/2} (2J+1) (2J'+1) Y_{lm_i}^* Y_{l'm'_i} \begin{pmatrix} j & l & J \\ \Omega & 0 & -\Omega \end{pmatrix} \begin{pmatrix} j & l & J \\ m & m_l & -M \end{pmatrix} \\ & \times \begin{pmatrix} j & l' & J' \\ \Omega' & 0 & -\Omega' \end{pmatrix} \begin{pmatrix} j & l' & J' \\ m' & m'_l & -M' \end{pmatrix} \begin{pmatrix} J & 1 & J_i \\ M & \eta & -M_i \end{pmatrix} \begin{pmatrix} J & 1 & J_i \\ \Omega & q & -\Omega_i \end{pmatrix} \\ & \times \begin{pmatrix} J' & 1 & J_i \\ M' & \eta' & -M_i \end{pmatrix} \begin{pmatrix} J' & 1 & J_i \\ \Omega' & q' & -\Omega'_i \end{pmatrix} M_{j\Omega, \Omega'} (M_{j\Omega, \Omega'})^*, \end{aligned} \quad (\text{A5})$$

where $M_{j\Omega, \Omega'}$ is the transition matrix element defined in Eq. (8). The product of the spherical harmonics in Eq. (A5) can be written as a sum of spherical harmonic functions Y_{S-s} by using the Clebsch–Gordan series.⁸ Then Eq. (A5) can be further simplified by summing over M_i and m'_i by use of Eq. (4.16) of Ref. 8,

$$\begin{aligned} \begin{pmatrix} j_1 & j_2 & j_3 \\ m_1 & m_2 & -m_3 \end{pmatrix} \begin{pmatrix} j_4 & j_5 & j_6 \\ m_4 & m_5 & m_3 \end{pmatrix} = & \sum_{j_6} (2j_6+1) (-1)^{j_1+j_2-j_3+j_4+j_5+j_6-m_1-m_4} \\ & \times \begin{pmatrix} j_1 & j_2 & j_3 \\ j_4 & j_5 & j_6 \end{pmatrix} \begin{pmatrix} j_5 & j_1 & j_6 \\ m_5 & m_1 & m_6 \end{pmatrix} \begin{pmatrix} j_2 & j_4 & j_6 \\ m_2 & m_4 & -m_6 \end{pmatrix}. \end{aligned} \quad (\text{A6})$$

After calculation it results

$$\begin{aligned} \sigma_{m'm} = & \frac{2\pi^{3/2}\omega}{c} \sum_{lm_i} \sum_{l'} \sum_{\Omega JM} \sum_{\Omega' J' M'} \sum_{\Omega_i \Omega'_i} \sum_{Pp} \sum_{Ss} \sum_{Rr} (-1)^{J_i - \Omega_i - \Omega'_i - \Omega - \Omega' + P - m_l + S + l + R} (2l+1) (2l'+1) (2J+1) (2J'+1) \\ & \times (2R+1) (2S+1)^{1/2} (2P+1)^{1/2} Y_{S-s} E_{Pp} \begin{Bmatrix} J & 1 & J_i \\ 1 & J' & P \end{Bmatrix} \\ & \times \begin{Bmatrix} S & l & l' \\ J' & j & R \end{Bmatrix} \begin{pmatrix} j & l & J \\ \Omega & 0 & -\Omega \end{pmatrix} \begin{pmatrix} j & l & J \\ m & m_l & -M \end{pmatrix} \begin{pmatrix} j & l' & J' \\ \Omega' & 0 & -\Omega' \end{pmatrix} \begin{pmatrix} l & l' & S \\ 0 & 0 & 0 \end{pmatrix} \begin{pmatrix} J & J' & P \\ M & -M' & -P \end{pmatrix} \\ & \times \begin{pmatrix} J' & l & R \\ -M' & m_l & r \end{pmatrix} \begin{pmatrix} S & j & R \\ -s & m' & -r \end{pmatrix} \begin{pmatrix} J & 1 & J_i \\ \Omega & q & -\Omega_i \end{pmatrix} \begin{pmatrix} J' & 1 & J_i \\ \Omega' & q' & -\Omega'_i \end{pmatrix} M_{j\Omega, \Omega'} (M_{j\Omega, \Omega'})^* \end{aligned} \quad (\text{A7})$$

with the polarization function E_{Pp} being defined by Eq. (6). The summations over M , M' , and m_l are performed by applying Eq. (4.15) from Ref. 8, which is

$$\begin{aligned} \begin{pmatrix} j_1 & j_2 & j_3 \\ j_4 & j_5 & j_6 \end{pmatrix} \begin{pmatrix} j_5 & j_1 & j_6 \\ m_5 & m_1 & m_6 \end{pmatrix} = & \sum_{m_2, m_3, m_4} (-1)^{j_1+j_2-j_3+j_4+j_5+j_6-m_1-m_4} \\ & \times \begin{pmatrix} j_1 & j_2 & j_3 \\ m_1 & m_2 & -m_3 \end{pmatrix} \begin{pmatrix} j_4 & j_5 & j_6 \\ m_4 & m_5 & m_3 \end{pmatrix} \begin{pmatrix} j_2 & j_4 & j_6 \\ m_2 & m_4 & -m_6 \end{pmatrix}. \end{aligned} \quad (\text{A8})$$

The summations over l and l' can subsequently be carried out by the use of Eq. (A6) with the result

$$\begin{aligned} \sigma_{m'm} = & \frac{2\pi^{3/2}\omega}{c} \sum_{\Omega J} \sum_{\Omega' J'} \sum_{\Omega_i \Omega'_i} \sum_{Pp} \sum_{Ss} \sum_{Rr} (-1)^{J_i - \Omega_i - \Omega'_i + \Omega' + P + 2R} (2J+1) (2J'+1) (2R+1) (2S+1)^{1/2} (2P+1)^{1/2} \\ & \times Y_{S-s} E_{Pp} \times \begin{Bmatrix} J & 1 & J_i \\ 1 & J' & P \end{Bmatrix} \begin{pmatrix} j & R & P \\ m & -r & -p \end{pmatrix} \begin{pmatrix} j & S & R \\ m' & -s & -r \end{pmatrix} \begin{pmatrix} j & S & R \\ \Omega' & 0 & -\Omega' \end{pmatrix} \begin{pmatrix} J & J' & P \\ \Omega & -\Omega' & q-q' \end{pmatrix} \\ & \times \begin{pmatrix} R & j & P \\ \Omega' & -\Omega & q'-q \end{pmatrix} \begin{pmatrix} J & 1 & J_i \\ \Omega & q & -\Omega_i \end{pmatrix} \begin{pmatrix} J' & 1 & J_i \\ \Omega' & q' & -\Omega'_i \end{pmatrix} M_{j\Omega, \Omega'} (M_{j\Omega, \Omega'})^*. \end{aligned} \quad (\text{A9})$$

The multipoles T_{KQ} as defined by Eq. (3b) are now calculated by substitution of Eq. (A9) into Eq. (3b). The summation over m , m' , and r is then carried out by using Eq. (A8). The summations over R and J in the resulting equation is performed by using Eq. (A6). The summation over J' can then be done by applying the orthogonality property of the $3-j$ symbols. The final result is

$$T_{KQ} = \frac{2\pi^{3/2}\omega}{c} (2K+1)^{1/2} \sum_{\Omega\Omega'} \sum_{\Omega_i} \sum_{Pp} \sum_{Ss} (-1)^{j+2\Omega-\Omega_i+S+s+P+p} (2S+1)^{1/2} (2P+1)^{1/2} \\ \times Y_{S-s} E_{Pp} \begin{pmatrix} P & S & K \\ -p & s & Q \end{pmatrix} \begin{pmatrix} 1 & 1 & P \\ q' & -q & q-q' \end{pmatrix} \begin{pmatrix} j & j & K \\ -\Omega & \Omega' & q'-q \end{pmatrix} \begin{pmatrix} P & S & K \\ q'-q & 0 & q-q' \end{pmatrix} M_{j\Omega,\Omega'} (M_{j\Omega,\Omega'})^* \quad (\text{A10})$$

With the definitions given in Eqs. (5) and (7), Eq. (A10) reduces to Eq. (4).

APPENDIX B: RELATION WITH THE SEMICLASSICAL BIPOLAR MOMENTS

In the semiclassical limit of $j \gg J$, the projection m of \mathbf{j} on the space-fixed Z axis may be considered to vary continuously and one can write

$$\sigma_{mm}(\Theta_k, \Phi_k) \approx \frac{d^2\sigma}{d\omega_k d\omega_j}, \quad (\text{B1})$$

where $d\omega_k$ denotes the volume element corresponding with the polar angles of ejection (Θ_k, Φ_k) , while ω_j corresponds to that for polar angle (Θ_j, Φ_j) between \mathbf{j} and the body-fixed z axis (see Fig. 1). For large values of j the $3-j$ symbol in Eq. (3a) can be written as²⁴

$$\begin{pmatrix} j & K & j \\ -m & Q & m' \end{pmatrix} = \frac{(-1)^{j-K-m'}}{\sqrt{2j+1}} \delta_{Q,m-m'} D_{Q0}^K(\Phi_j, \Theta_j, 0). \quad (\text{B2})$$

The bipolar harmonics are defined as^{7,8,25}

$$B_{Pp}(K, S; \Theta_j, \Phi_j, \Theta_k, \Phi_k) \\ = \sum_Q (-1)^{P-p} \times (2P+1)^{1/2} \frac{4\pi}{(2K+1)^{1/2} (2S+1)^{1/2}} \\ \times \begin{pmatrix} K & P & S \\ Q & -p & s \end{pmatrix} Y_{KQ}(\Theta_j, \Phi_j) Y_{S-s}(\Theta_k, \Phi_k). \quad (\text{B3})$$

Note that the summation in Eq. (B3) reduces to only one term, since in Eq. (B2) $m=m'$, implying $Q=0$, while $p=0$ for the choice of the space-fixed frame made in this work. Combination of Eqs. (3) and (B1) to (B3) together with Eq. (A10) provides

$$\frac{d^2\sigma}{d\omega_k d\omega_j} \\ = \frac{4\pi^2\omega}{c} \sum_{Pp} \sum_K \sum_S B_{Pp}(K, S; \Theta_j, \Phi_j, \Theta_k, \Phi_k) (-1)^{K+S+s} \\ \times \frac{(2K+1)(2S+1)}{4\pi\sqrt{2j+1}} E_{Pp}(\mathbf{e}) \sum_{qq'} (-1)^q \\ \times \begin{pmatrix} 1 & 1 & P \\ q' & -q & q-q' \end{pmatrix} \begin{pmatrix} P & S & K \\ q'-q & 0 & q-q' \end{pmatrix} f_K(q, q') \quad (\text{B4})$$

which can be written as

$$\frac{d^2\sigma}{d\omega_k d\omega_j} = \frac{\sigma_0}{16\pi^2} \sum_{Pp} \sum_{KS} (2K+1)(2S+1) \\ \times b_p^P(K, S) B_{Pp}(K, S; \Theta_j, \Phi_j, \Theta_k, \Phi_k). \quad (\text{B5})$$

The coefficients $b_p^P(K, S)$ are the bipolar moments¹² and in the present notation they are given by

$$b_p^P(K, S) = \frac{8\pi^2\omega}{\sigma_0 c} (-1)^{K+S+s} \frac{1}{(2j+1)^{1/2}} E_{Pp}(\mathbf{e}) \\ \times \sum_{qq'} (-1)^q \begin{pmatrix} 1 & 1 & P \\ q' & -q & q-q' \end{pmatrix} \\ \times \begin{pmatrix} P & S & K \\ q'-q & 0 & q-q' \end{pmatrix} f_K(q, q'), \quad (\text{B6})$$

where σ_0 is the angular integrated cross section.

Equation (B6) provides the relationship between the general form of the semiclassical excitation matrix [Eq. (B5)] and the detailed quantum matrix elements of the transition dipole through the functions $f_K(q, q')$ defined in Eq. (7). The functions $f_K(q, q')$ can relate to incoherent terms ($q=q'$) as well as coherent terms ($|q-q'|=1$ or $|q-q'|=2$). In the semiclassical limit $j \gg J$, and thus $j \gg \Omega$, the angle between \mathbf{j} and the recoil direction of the photofragments is $\Theta_j = \Pi/2$. Using the semiclassical approximation (B2) in Eq. (7) yields

$$f_K(q, q') = \frac{(-1)^K}{\sqrt{2j+1}} \delta_{q'-q, \Omega'-\Omega} D_{q'-q, 0}^K \times (0, \pi/2, 0) M_{j\Omega, \Omega'} (M_{j\Omega, \Omega'})^*, \quad (\text{B7})$$

and it is concluded that in the semiclassical limit, the functions $f_K(q, q')$ are different from zero when $|q - q'| = 0$, or 2, for K even, and when $|q - q'| = 1$ for K odd. These results provide the relationship between the quantum theory and the semiclassical treatment provided by Dixon.¹²

¹See, for instance, the contributions in *Dynamical Stereochemistry Issues*: (a) *J. Phys. Chem.* **91**, 5365 (1987); (b) *J. Chem. Soc. Faraday Trans. 2* **85**, 925 (1989); (c) **89**, 1401 (1993).

²(a) R. N. Zare, *Ber. Bunsenges. Phys. Chem.* **86**, 422 (1982); (b) H. Reiser and C. Wittig, *Annu. Rev. Phys. Chem.* **37**, 307 (1986); (c) P. L. Houston, *J. Phys. Chem.* **91**, 5388 (1987); (d) J. P. Simons, *ibid.* **91**, 5378 (1987); (e) G. E. Hall and P. L. Houston, *Annu. Rev. Phys. Chem.* **40**, 375 (1989); (f) F. J. Comes, *Ber. Bunsenges. Phys. Chem.* **94**, 1268 (1990); (g) R. N. Dixon, *Acc. Chem. Res.* **24**, 16 (1991); (h) M. N. R. Ashfold, I. R. Lambert, D. H. Mordaunt, G. P. Morley, and C. M. Western, *J. Phys. Chem.* **96**, 2938 (1992); (i) I. Powis, in *Dynamical Processes in Molecular Physics*, edited by G. Delgado-Barrio (IOP, Bristol, 1993).

³(a) J. Vigué, P. Grangier, G. Roger, and A. Aspect, *J. Phys. Lett.* **42**, L531 (1981); (b) J. Vigué, J. A. Beswick, and M. Broyer, *J. Phys. (Paris)* **44**, 1225 (1983); (c) J. Vigué, B. Girard, G. Gouédard, and N. Billy, *Phys. Rev. Lett.* **62**, 1358 (1989); (d) D. V. Kupriyanov, B. N. Sevastianov, and O. S. Vasyutinskii, *Z. Phys. D* **15**, 105 (1990); (e) J. A. Beswick, M. Glass-Maujean, and O. Roncero, *J. Chem. Phys.* **96**, 7514 (1992); (f) M. R. Wedlock and K. F. Freed, *ibid.* **95**, 7275 (1991); (g) M. R. Wedlock, E. Jensen, L. J. Butler, and K. F. Freed, *J. Phys. Chem.* **95**, 8096 (1991); (h) M. Dantus, R. M. Bowman, J. S. Baskin, and A. H. Zewail, *Chem. Phys. Lett.* **159**, 406 (1989).

⁴(a) E. Hasselbrink, J. R. Waldeck, and R. N. Zare, *Chem. Phys.* **126**, 191 (1988); (b) M. Mons and I. Dimicoli, *J. Chem. Phys.* **90**, 4037 (1989); (c) J. F. Black, J. R. Waldeck, and R. N. Zare, *ibid.* **92**, 3519 (1990); (d) C. A. Taatjes, M. H. M. Janssen, and S. Stolte, *Chem. Phys. Lett.* **203**, 363 (1993); (e) Y. Naitoh, Y. Fujimura, K. Honma, and O. Kajimoto, *ibid.* **205**, 423 (1993); (f) D. David, I. Bar, and S.

Rosenwaks, *J. Chem. Phys.* **99**, 4218 (1993); (g) C. J. K. Quayle, I. M. Bayle, E. Takács, X. Chen, K. Burnett, and D. M. Segal, *ibid.* (in press).

⁵(a) U. Fano, *Rev. Mod. Phys.* **29**, 74 (1957); (b) U. Fano and J. H. Macek, *ibid.* **45**, 553 (1973).

⁶W. Happer, *Rev. Mod. Phys.* **44**, 169 (1972).

⁷K. Blum, *Density Matrix Theory and Applications* (Plenum, New York, 1981).

⁸R. N. Zare, *Angular Momentum* (Wiley, New York, 1988).

⁹C. H. Greene and R. N. Zare, *Annu. Rev. Phys. Chem.* **33**, 119 (1982).

¹⁰S. J. Singer, K. F. Freed, and Y. B. Band, *J. Chem. Phys.* **79**, 6060 (1983).

¹¹M. Glass-Maujean and J. A. Beswick, *J. Chem. Soc. Faraday Trans. 2* **85**, 983 (1989).

¹²R. N. Dixon, *J. Chem. Phys.* **85**, 1866 (1986).

¹³G. E. Hall, Sivakumar, P. L. Houston, and I. Burak, *Phys. Rev. Lett.* **56**, 1671 (1986).

¹⁴(a) K. L. Reid, D. J. Leahy, and R. N. Zare, *J. Chem. Phys.* **95**, 1746 (1991); (b) D. J. Leahy, K. L. Reid, H. Park, and R. N. Zare, *ibid.* **97**, 4948 (1992).

¹⁵(a) N. A. Cherepkov, *Adv. At. Mol. Phys.* **19**, 395 (1983); (b) A. V. Golovin, V. V. Kuznetsov, and N. A. Cherepkov, *Sov. Tech. Phys. Lett.* **16**, 363 (1990); (c) M. Büchner, G. Raseev, and N. A. Cherepkov, *J. Chem. Phys.* **96**, 2691 (1992).

¹⁶U. Heinzmann, in *Applications of Circularly Polarized Radiation Using Synchrotron Radiation and Ordinary Sources*, edited by F. Allen and C. Bustamante (Plenum, New York, 1985).

¹⁷R. N. Zare, *Mol. Photochem.* **4**, 1 (1972).

¹⁸E. E. Nikitin and S. Y. Umanskii, *Theory of Slow Atomic Collisions* (Springer, Berlin, 1984).

¹⁹G. G. Balint-Kurti and M. Shapiro, *Chem. Phys.* **61**, 137 (1981); *Adv. Chem. Phys.* **60**, 403 (1985).

²⁰D. V. Kupriyanov and O. S. Vasyutinskii, *Chem. Phys.* **171**, 25 (1993).

²¹O. S. Vasyutinskii, *Sov. Phys. JETP* **54**, 855 (1981); *Khim. Fis. (USSR)* **5**, 768 (1986).

²²O. S. Vasyutinskii, *Opt. Spectrosc.* **54**, 524 (1983).

²³M. Glass-Maujean and J. A. Beswick, *Phys. Rev. A* **36**, 1170 (1987).

²⁴D. A. Varshalovich, A. N. Moskalev, and V. K. Khersonskii, *Quantum Theory of Angular Momentum* (World Scientific, Singapore, 1988).

²⁵(a) J. M. Brown and B. J. Howard, *Mol. Phys.* **31**, 1517 (1976); (b) **32**, 1197 (1976).